FISHERIES OCEANOGRAPHY

FISHERIES OCEANOGRAPHY Fish. Oceanogr. 25:3, 277–291, 2016

Natal origin and population connectivity of bigeye and yellowfin tuna in the Pacific Ocean

JAY R. ROOKER,[1,2]* R. J. DAVID WELLS,[1,2] DAVID G. ITANO,[3] SIMON R. THORROLD[4] AND JESSICA M. LEE[1]

[1]*Department of Marine Biology, Texas A&M University at Galveston, 1001 Texas Clipper Road, Galveston, TX 77554, U.S.A.*

[2]*Department of Wildlife and Fisheries Sciences, Texas A&M University, College Station, TX 77843, U.S.A.*

[3]*National Marine Fisheries Service, Pacific Islands Region, 1601 Kapiolani Boulevard, Suite 1110, Honolulu, HI 96814, U.S.A.*

[4]*Biology Department, Woods Hole Oceanographic Institution, Woods Hole, MA 02543, U.S.A*

ABSTRACT

Natural chemical markers (stable isotopes and trace elements) in otoliths of bigeye tuna (*Thunnus obesus*) and yellowfin tuna (*T. albacares*) were used to investigate their origin and spatial histories in the western and central Pacific Ocean (WCPO). Otolith chemistry of young-of-the-year (YOY) *T. obesus* and *T. albacares* from four regions in the WCPO was first determined and used to establish baseline chemical signatures for each region. Spatial variation in stable isotope ratios of YOY *T. obesus* and *T. albacares* was detected, with the most noticeable difference being depleted otolith $\delta^{18}O$ values for both species from the far west equatorial and west equatorial regions relative to the central equatorial and Hawaii regions. Elemental ratios in otoliths were also quantified for YOY *T. obesus* and *T. albacares* collected in 2008, and several showed promise for distinguishing YOY *T. obesus* (Mg:Ca, Mn:Ca, and Ba:Ca) and *T. albacares* (Li:Ca and Sr:Ca). The natal origin of age-1 to age-2+ *T. obesus* and *T. albacares* was then determined for two regions of the WCPO, and mixed-stock analysis indicated that *T. obesus* and *T. albacares* in our west equatorial sample were almost entirely from local production, with a minor contribution from central equatorial waters. Similarly, *T. albacares* collected in Hawaii were exclusively from local sources; however, a large fraction of *T. obesus* in Hawaii were classified to the central equatorial region, suggesting that the movement of migrants from outside production zones (i.e., south of Hawaii) are important to Hawaii's domestic fishery.

Key words: equatorial Pacific, isotopes, migration, natal origin, otolith chemistry, pelagic, stable isotopes, trace elements, stock mixing

INTRODUCTION

Pelagic fishes that utilize open-ocean ecosystems are capable of long-distance migrations that often cross international jurisdictions or ocean boundaries (Rooker *et al.*, 2008a, 2014; Block *et al.*, 2011). Unfortunately, migratory behaviors as well as residency patterns of many pelagic fishes are poorly understood, limiting our ability to effectively manage and conserve certain populations (Rooker *et al.*, 2014). This is particularly true for tropical tunas, which are important predators in open-ocean ecosystems (Young *et al.*, 2010; Ferriss and Essington, 2011), and represent key components of high seas fisheries in tropical waters (Joseph *et al.*, 2010). Fishing pressure and harvest scenarios for tropical tunas commonly vary spatially within an ocean basin, and, therefore, the population dynamics of these stocks will be influenced by their movement patterns (Sibert and Hampton, 2003).

Several species of tropical tunas occur in the western and central Pacific Ocean (WCPO), and even though these tunas are capable of undertaking long-distance migrations (> 1000 km), restricted movements and high site fidelity have also been reported (Hampton and Gunn, 1998; Itano and Holland, 2000; Schaefer *et al.*, 2011, 2015). Defining natal origins, stock structure and migration routes of tropical tunas in the WCPO is critical for their management, particularly for two species heavily targeted by fishing fleets: bigeye tuna (*Thunnus obesus*) and yellowfin tuna (*T. albacares*) (Schaefer, 2008). Results to date indicate that total and adult spawning stock biomass of *T. obesus* and *T. albacares* in the WCPO have declined significantly over the past few decades with catches now predicted to be close to or exceeding the

*Correspondence. e-mail: rookerj@tamug.edu

Received 12 August 2015

Revised version accepted 20 January 2016

maximum sustainable yield (Davies *et al.*, 2014; Harley *et al.*, 2014). These apparent population declines are of particular concern because the stock structure, migration patterns and the degree of mixing within the WCPO for both species are unresolved. Several approaches have been used to investigate the movement and mixing rates of *T. obesus* and *T. albacares* from different production areas in the WCPO, and some degree of stock or contingent structure may be present in both species (Schaefer *et al.*, 2011, 2015). Still, data are currently insufficient to move away from the premise of a 'single' panmictic population for both *T. obesus* and *T. albacares* (Ward *et al.*, 1997; Grewe and Hampton, 1998), even though data from tagging and genetics research suggests that tropical tunas display more site fidelity and potentially exist as discrete subpopulations or management units within the WCPO (Hampton and Gunn, 1998; Itano and Holland, 2000; Sibert and Hampton, 2003; Grewe *et al.*, 2015; Schaefer *et al.*, 2015).

In the present study, we examined the origin and movement of young (age-1 to age-2+) *T. obesus* and *T. albacares* in the WCPO using chemical markers (stable isotopes and trace elements) in their otoliths (ear stones). Similar to other highly mobile species, understanding movement patterns is of particular interest because the potential for basin-scale migration is high for young tunas (e.g., Rooker *et al.*, 2008b). Natural chemical markers, particularly stable oxygen and carbon isotopes (δ^{18}O and δ^{13}C), have been used previously to determine the natal origin and migration patterns of both tropical and temperate tunas (Rooker *et al.*, 2003, 2008a, 2014; Wells *et al.*, 2012), and the current application relied on the development of baseline chemical signatures in the otoliths of young-of-the-year (YOY) *T. obesus* and *T. albacares* from different regions in the WCPO. After the characterization of baseline signatures, region-specific estimates of natal origin were determined by comparing δ^{18}O and δ^{13}C values in the otolith cores of age-1 to age-2+ *T. obesus* and *T. albacares* (corresponding to otolith material deposited during the YOY period) to our baseline sample for each species.

METHODS

YOY *T. obesus* and *T. albacares* were collected from four geographic regions in the WCPO: (i) far west equatorial (Philippines, Indonesia), (ii) west equatorial (Marshall Islands, Solomon Islands), (iii) central equatorial (Line Islands, French Polynesia) and (iv) Hawaii [Hawaii (Island), Maui, Oahu, Kauai, Cross Seamount] (Fig. 1). Our baselines were comprised of YOY *T. obesus* and *T. albacares* sampled in late 2007 to mid-2008 and late 2008 to mid-2009, referred to hereafter as 2008 and 2009, respectively (Table 1). Within each presumed spawning/nursery area, specimens were sampled from multiple collection dates and locations to obtain a representative baseline sample for each species. Age-1 to age-2+ *T. obesus* and *T. albacares* of an unknown natal origin were collected in 2009–2010 from the west equatorial Pacific (Marshall Islands) and Hawaii regions (Table 1). In the present study, *T. obesus* and *T. albacares* ranging in size from 20 to 60 cm fork length (FL) and 70 to 120 cm FL were classified as YOY (~3–12 months old) and age-1 to age-2+, respectively (Lehodey and Leroy, 1999; Lehodey *et al.*, 1999).

Sagittal otoliths were extracted from both fresh and frozen *T. obesus* and *T. albacares*, cleaned of biological tissue and stored dry. One sagittal otolith from each tuna was embedded in Struers EpoFix resin (Struers A/S, Ballerup, Denmark) and sectioned using a low-speed ISOMET saw (Beuhler, Lake Bluff, IL, USA) to

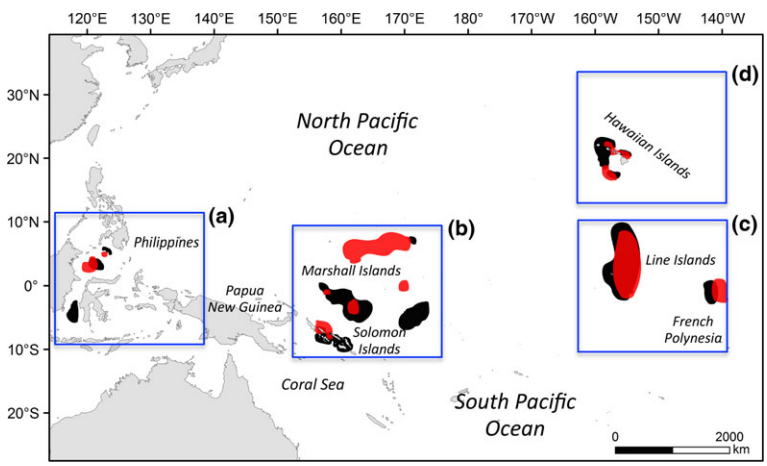

Figure 1. Map of the four regions sampled for bigeye tuna (*Thunnus obesus)* and yellowfin tuna (*T. albacares*) in the western and central Pacific Ocean (WCPO): (a) far west equatorial (Philippines, Indonesia), (b) west equatorial (Marshall Islands, Solomon Islands), (c) central equatorial (Line Islands, French Polynesia) and (d) Hawaii (Hawaii, Maui, Oahu, Kauai, Cross Seamount). Collection areas for *T. obesus* (red) and *T. albacares* (black) in the WCPO denoted.

Table 1. Summary data for bigeye tuna (*Thunnus obesus)* and yellowfin tuna (*T. albacares*) collected in the four regions of the western and central Pacific Ocean (WCPO).

Region	Location(s)	Year	Age	N	FL cm (SD)
T. obesus					
A	Philippines	2008	YOY	18	27.7 (4.1)
		2009	YOY	22	30.0 (5.4)
B	Marshall & Solomon Islands	2008	YOY	34	32.8 (3.1)
		2009	YOY	0	
C	Line Islands/French Polynesia	2008	YOY	25	48.3 (6.2)
		2009	YOY	41	45.8 (4.4)
D	Maui/Oahu/Kauai/Cross	2008	YOY	42	51.6 (6.1)
		2009	YOY	7	54.4 (5.1)
B	Marshall Islands	2009–2010	1–2+	50	110.7 (6.5)
D	Maui/Oahu/Kauai/Cross	2009–2010	1–2+	42	75.7 (10.8)
T. albacares					
A	Philippines/Indonesia	2008	YOY	25	26.0 (3.5)
		2009	YOY	29	32.2 (4.4)
B	Marshall & Solomon Islands	2008	YOY	50	32.9 (3.1)
		2009	YOY	16	53.9 (2.9)
C	Line Islands/French Polynesia	2008	YOY	25	52.3 (2.2)
		2009	YOY	18	46.9 (4.1)
D	Maui/Oahu/Kauai/Cross	2008	YOY	62	44.5 (9.2)
		2009	YOY	43	39.7 (8.0)
B	Marshall Islands	2009–2010	1–2+	50	112.9 (4.6)
D	Maui/Oahu/Kauai/Cross	2009–2010	1–2+	62	79.1 (9.4)

(A) far west equatorial (Philippines, Indonesia), (B) west equatorial (Marshall Islands, Solomon Islands), (C) central equatorial (Line Islands, French Polynesia) and (D) Hawaii (Hawaii, Maui, Oahu, Kauai, Cross Seamount). Collection data for age-1 to 2+ *T. obesus* and *T. albacares* collected in two regions (west equatorial and Hawaii) are also shown. The mean fork length (cm) and range provided by region and year.

obtain a 1.5 mm transverse section that included the otolith core. Otolith sections were then attached to a sample plate using Crystalbond™ thermoplastic glue (SPI Supplies/Structure Probe Inc., West Chester, PA, USA), and the region corresponding to the early portion of the YOY period was isolated and powdered using a New Wave Research MicroMill (Fremont, CA, USA). Similar to Wells *et al.* (2012), the template was constructed using otolith measurements from the smallest individuals [≤ 25 cm fork length (FL)] in our sample of each species, which represented core material accreted during the first ~3 months of life. The final milling template was the same for *T. obesus* and *T. albacares*, and a series of drill passes was run over the preprogrammed milling template using a 500-μm-diameter Brasseler carbide bit (Brasseler USA, Medical L.L.C., Ventura, CA, USA) until a depth of approximately 800 μm was reached. The powdered core material was transferred to silver capsules for stable isotope analysis.

Otolith $\delta^{18}O$ and $\delta^{13}C$ values for YOY *T. obesus* and *T. albacares* were determined using an automated carbonate preparation device (KIEL-III; Thermo Fisher Scientific, Inc., Waltham, MA, USA) coupled to an isotope ratio monitoring mass spectrometer (Finnigan MAT 252; Thermo Fisher Scientific, Inc.) at the University of Arizona Environmental Isotope Laboratory. Powdered otolith samples were reacted with dehydrated phosphoric acid under vacuum at 70 °C. The isotope ratio measurement was calibrated based on repeated measurements of the National Bureau of Standards (NBS), NBS-19 and NBS-18, with 6 standards run for every 40 samples; precision was approximately ± 0.11‰ and ± 0.08‰ for $\delta^{18}O$ and $\delta^{13}C$, respectively. Otolith $\delta^{18}O$ and $\delta^{13}C$ values are reported relative to the Vienna Pee Dee Belemnite (VPDB) scale after comparison to an in-house laboratory standard calibrated to VPDB.

Elemental chemistry was determined using either a solution-based or laser ablation (LA) approach on an inductively coupled plasma-mass spectrometer (ICP-MS). Because the goal for this component of the investigation was to determine whether the addition of elements improved our ability to distinguish YOY

T. obesus and *T. albacares* from different regions, the other sagittal otolith from a subset of the individuals used for otolith $\delta^{18}O$ and $\delta^{13}C$ analysis was included in ICP-MS runs. Solution-based ICP-MS was performed on *T. obesus* otoliths using the Agilent HP 4500 quadrupole ICP-MS at the University of Maryland Center for Environmental Science, Chesapeake Biological Laboratory. The whole otolith approach provided an integrated measure of the entire YOY period. Otoliths were first cleaned with doubly deionized water ($DDIH_2O$) and hydrogen peroxide (H_2O_2), immersed briefly (1 min) in dilute nitric acid (HNO_3) to remove surface contamination, and then dried under a laminar flow clean fume hood. In preparation for instrument analysis, each otolith was weighed to the nearest 0.01 mg and placed in a clean, plastic centrifuge tube. Whole otoliths were then digested in concentrated HNO_3, and the quantities of acid used and volumes were proportional to the otolith weights. Digests were diluted with $DDIH_2O$ to a final acid concentration of 1% HNO_3. The levels of Ca and Sr were determined using otolith-certified reference material (CRM; Yoshinaga *et al.*, 2000), and four elemental ratios (Mg:Ca, Mn:Ca, Sr:Ca and Ba:Ca) in the whole otoliths of YOY *T. obesus* were estimated according to the method of standard additions. Instrument precision was assessed by running the CRM every 5 to 10 samples, and external precision (relative standard deviation) for this reference material was as follows: Mg:Ca = 10.6%, Mn:Ca = 8.7%, Sr:Ca = 1.8% and Ba:Ca = 18.9%. In contrast, otoliths of YOY *T. albacares* were processed with a LA ICP-MS at the Woods Hole Oceanographic Institution Plasma Mass Spectrometry Facility. The system consisted of a New Wave Research NWR 213 nm Nd:YAG laser system and a Thermo Element2 single collector ICP-MS. Ablation diameters were 60 μm, and the location of the early YOY period was based on otolith microstructure analysis. The first ablation spot was set at the otolith core (operationally defined as the narrowest part of the otolith section), followed by two equally spaced spots on each side of the core (n = 3 ablation spots per otolith). Ablation spots incorporated otolith material accreted during the first 3–4 months of life. The ablated material was transported via a Helium (He) gas stream to the dual-inlet quartz spray chamber where it was mixed with a 2% HNO_3 aerosol from a self-aspirating PFA 20 μL min^{-1} nebulizer, using Argon (Ar) as the sample gas, in the concentric part of the quartz dual-inlet spray chamber. A single isotope was measured from each of the five elements (^{7}Li, ^{25}Mg, ^{48}Ca, ^{55}Mn, ^{88}Sr and ^{138}Ba). We ran an instrument blank (2% HNO_3) and two otolith CRMs every nine samples. We blank-corrected raw isotope values by calculating a blank value for each sample using a linear interpolation between bracketed blanks. A dissolved otolith CRM (Sturgeon *et al.*, 2005), diluted to a Ca concentration of 40 $\mu g\ g^{-1}$, was used to correct for instrument isotope mass bias according to Walther *et al.* (2008). Instrument precision was assessed by running another CRM (Yoshinaga *et al.*, 2000), similarly dissolved and diluted to a Ca concentration of 40 $\mu g\ g^{-1}$. External precision (relative standard deviation) for this reference material ($n = 19$) was as follows: Li:Ca = 5.8%, Mg:Ca = 1.9%, Mn:Ca = 20.1%, Sr:Ca = 1.6% and Ba:Ca = 2.5%. For both solution-based and laser ablation ICP-MS runs, appropriate procedural blanks and reference material (e.g., NIST 614, NIST 915a) were used to estimate the recovery, precision and accuracy of analytical runs.

Analysis of variance (ANOVA) and multivariate analysis of variance (MANOVA) were used to test for regional differences in stable isotopes and element:Ca ratios of YOY *T. obesus* and *T. albacares*. MANOVA significance was based on Pillai's trace statistic, and significance for all ANOVA and MANOVA tests was based on an alpha level of 0.05. Canonical discriminant analysis (CDA) was used to display multivariate means of otolith chemistry data in a reduced space (two dimensions) for MANOVAs showing a significant region effect. Discriminant function coefficients were included on CDA plots as biplot vectors from a grand mean to show the discriminatory influence of stable isotopes or trace elements used in each model. Quadratic discriminant function analysis (QDFA) was then used to determine the classification accuracy of YOY *T. obesus* and *T. albacares* to each nursery (n = 4) using otolith chemistry. In addition, QDFA was used to determine the classification accuracy of both species to broader regions (e.g., west equatorial Pacific versus central Pacific). QDFA is the preferred approach when the variance-covariance matrix of our predictor variables differs. In addition, we opted for QDFA because it does not have the homogeneity of covariance matrices assumption and is robust to moderate deviations from normality (McGarigal *et al.*, 2000).

Region-specific estimates of natal origin for *T. obesus* and *T. albacares* were estimated by comparing otolith core $\delta^{18}O$ and $\delta^{13}C$ values of age-1 to age-2+ tunas to $\delta^{18}O$ and $\delta^{13}C$ values from core material of YOY tunas in our baseline samples. The natal origin of *T. obesus* and *T. albacares* from two different regions of the WCPO (the Marshall Islands and the Hawaiian Islands) was determined using direct maximum likelihood estimation (MLE) and a classification-based

estimation (maximum classification likelihood, MCL) from the mixed-stock analysis program HISEA (Millar, 1990). We focus on MLE because the performance is typically superior to classification-based methods; however, classification-based methods such as MCL appear to be more robust than direct MLE to anomalies in baseline data (Millar, 1987, 1990), and thus results from this estimator are included for comparative purposes. Mix-stock analysis was run under the bootstrap mode to obtain standard deviations around estimated proportions (error terms) with 500 simulations. Prior to mixed-stock analysis, otolith δ^{18}O and δ^{13}C values of YOY (baseline) and age-1 to age-2+ *T. obesus* and *T. albacares* were plotted in ordination space to further evaluate whether all potential source populations (i.e., nurseries) were sampled in the WCPO (Chittaro *et al.*, 2009). A small percentage of otolith δ^{18}O and δ^{13}C values from our sample of age-1 to age-2+ tuna occurred outside the 95% confidence ellipse of the YOY baselines for each species (< 2%), and thus potential bias as a result of the presence of individuals from nurseries not sampled was assumed to be insignificant.

RESULTS

Variation in YOY signatures

Otolith δ^{18}O and δ^{13}C values for two cohorts (2008 and 2009) of YOY *T. obesus* and *T. albacares* were distinct among regions in the WCPO. A temporal effect was observed for otolith δ^{18}O, with mean values being statistically different between years in one region for *T. obesus* (far west equatorial) and two regions for *T. albacares* (far west equatorial, west equatorial) (ANOVA, $P < 0.05$; Table 2). Otolith δ^{18}O values of both species from far west equatorial waters were depleted by more than 0.2‰ in 2009 relative to 2008. No interannual effect in otolith δ^{18}O was observed for either species in the central equatorial or Hawaii region, with differences between years typically less than 0.1‰. A significant year effect on otolith δ^{13}C was also detected for *T. obesus* in the far west equatorial region, with more enriched values observed in 2009 (Table 2). No temporal effect on otolith δ^{13}C was observed for *T. albacares* and all four regions were statistically similar between 2008 and 2009.

Regional differences in otolith δ^{18}O for both YOY *T. obesus* and *T. albacares* were maintained when 2008 and 2009 cohorts were pooled, indicating that temporal variability was minor relative to geographic variability. The mean otolith δ^{18}O (± 1 SD) for *T. obesus* varied significantly among the four regions (ANOVA $P < 0.01$) and increased from west to east in equatorial waters: far west equatorial (−2.65 ± 0.20‰), west equatorial (−2.22 ± 0.22‰) and central equatorial (−1.85 ± 0.19‰) (Fig. 2). The Hawaii region (−1.94 ± 0.20‰) was most similar to the central equatorial, with the mean difference being less than 0.1‰ and overlapping 95% confidence limit (CL) ellipses around multivariate means from CDA (Fig. 3). The otolith δ^{18}O for YOY *T. albacares* also varied regionally (ANOVA $P < 0.01$) and displayed a similar pattern to *T. obesus* with values increasing from west to east: far west equatorial

Table 2. Mean otolith δ^{18}O and δ^{13}C values for young-of-the year (YOY) bigeye tuna (*Thunnus obesus*) and yellowfin tuna (*T. albacares*) collected in 2008 and 2009 from four regions of the western and central Pacific Ocean (WCPO).

	2008			2009			Difference			
Region	δ^{13}C	δ^{18}O	N	δ^{13}C	δ^{18}O	N	δ^{13}C	p	δ^{18}O	*P*
T. obesus										
A	−10.29	−2.49	18	−9.58	−2.76	22	0.71	**	0.27	**
B	−9.77	−2.29	34			0				
C	−9.72	−1.88	25	−9.65	−1.84	41	0.07	**	0.04	ns
D	−9.39	−1.96	42	−10.08	−1.94	7	0.69	NS	0.02	ns
T. albacares										
A	−10.56	−2.65	25	−10.30	−2.87	29	0.26	NS	0.22	**
B	−9.47	−2.51	50	−9.32	−2.37	16	0.15	NS	0.14	**
C	−9.72	−2.13	25	−9.61	−2.18	18	0.11	NS	0.05	ns
D	−9.71	−1.95	62	−9.74	−1.69	43	0.03	NS	0.26	ns

A = far west equatorial, B = west equatorial, C = central equatorial, D = Hawaii. Mean difference in otolith δ^{18}O and δ^{13}C between years is shown along with results of ANOVA (NS = non significant, $^{**}P < 0.01$). Sample sizes (N) provided.

Figure 2. Contour plots of otolith $\delta^{18}O$ and $\delta^{13}C$ for young-of-the-year (YOY) bigeye tuna (*Thunnus obesus)* and yellowfin tuna (*T. albacares*) from the four regions of the western and central Pacific Ocean (WCPO): (a) far west equatorial, (b) west equatorial, (c) central equatorial and (d) Hawaii. Bivariate kernel density estimated at four levels (25%, 50%, 75% and 100%).

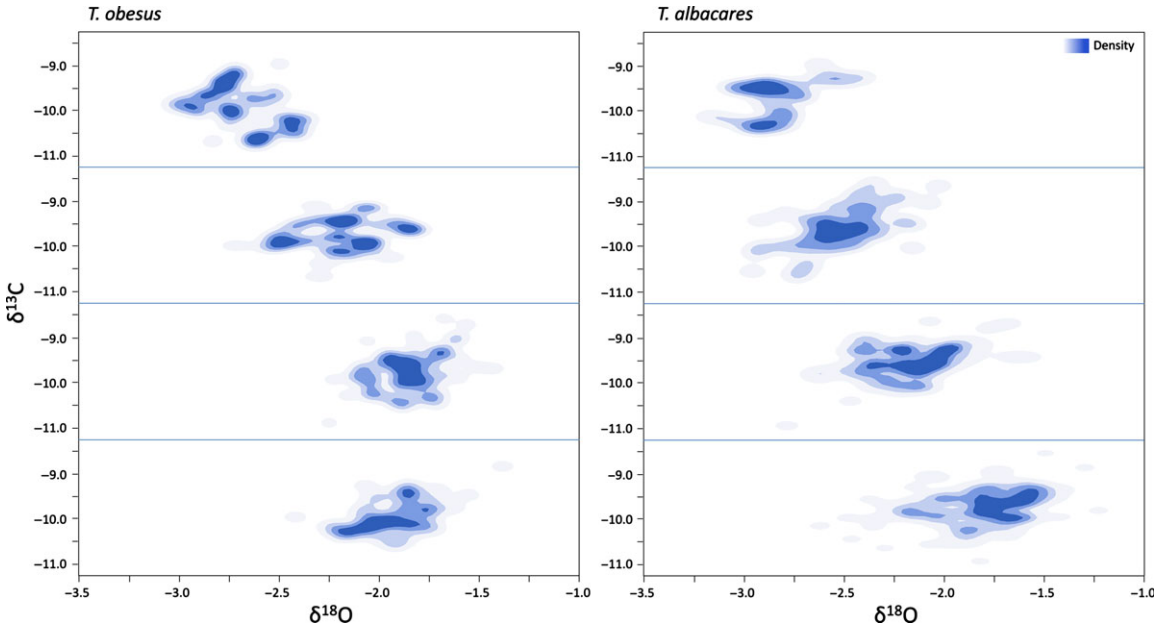

(−2.77 ± 0.26‰), west equatorial (−2.48 ± 0.21‰) and central equatorial (−2.14 ± 0.25‰). In contrast to *T. obesus*, otolith $\delta^{18}O$ for *T. albacares* in the two central regions was different, with the Hawaii region (−1.83 ± 0.26‰) being enriched by approximately 0.3% relative to the central equatorial region. Multivariate means and 95% CL ellipses for all four regions were clearly separated on the CDA plot, and similar to *T. obesus*, biplot vectors on CDA indicated that regional discrimination was strongly influenced by $\delta^{18}O$ (Fig. 3).

Otolith $\delta^{13}C$ for YOY *T. obesus* was statistically similar among the four regions (ANOVA $P > 0.05$), and CDA vectors indicated that $\delta^{13}C$ was marginally important in separating regions (Fig. 3). Mean values (± 1 SD) for all regions were remarkably similar and within 0.2‰: far west equatorial (−9.91 ± 0.49‰), west equatorial (−9.78 ± 0.38‰), central equatorial (−9.77 ± 0.49‰) and Hawaii (−9.93 ± 0.43‰). While otolith $\delta^{13}C$ was significantly different among the four regions sampled for *T. albacares* (ANOVA $P > 0.01$), the effect was due almost entirely to one region, the far west equatorial, with CDA plots showing that the multivariate mean for this region was strongly influenced by $\delta^{13}C$ (Fig. 3). Mean otolith $\delta^{13}C$ for *T. albacares* in this region (−10.42 ± 0.59‰) was depleted by more than 0.7‰ relative to all other regions sampled: west equatorial (−9.43 ± 0.47‰), central equatorial (−9.67 ± 0.44‰) and Hawaii (−9.67 ± 0.43‰).

QDFA parameterized with otolith $\delta^{18}O$ and $\delta^{13}C$ values indicated that the overall cross-validated classification success of YOY *T. obesus* to the four regions was 58% in 2008 (range: 48–84% by region). Samples were not available for one region (west equatorial) in 2009, and overall classification success to three regions in this year was 78% (range: 66–100%); QDFA using pooled 2008 and 2009 data resulted in an overall classification success of 61% (range: 52–80%). Regional discrimination of YOY *T. albacares* using otolith $\delta^{18}O$ and $\delta^{13}C$ was higher with an overall cross-validated success of 72% (range: 59–86%) and 84% (range: 81–90%) in 2008 and 2009, respectively; QDFA using pooled 2008 and 2009 data resulted in an overall classification success of 74% (range: 65–80%). For both species, the highest classification success was attributed to either the far west or west equatorial regions. When the western (far west and west equatorial) and central (central equatorial, Hawaii) locations were pooled, the overall classification success to these two larger regions improved to 82% in 2008 (range: 79–85%) and 100% in 2009 for *T. obesus* and 91% in 2008 (range: 88–95%) and 94% in 2009 (range: 89–98%) for *T. albacares*. Our ability to discriminate YOY *T. obesus* and *T. albacares* to regional nurseries was due primarily to otolith $\delta^{18}O$ (Figs 2 and 3), and

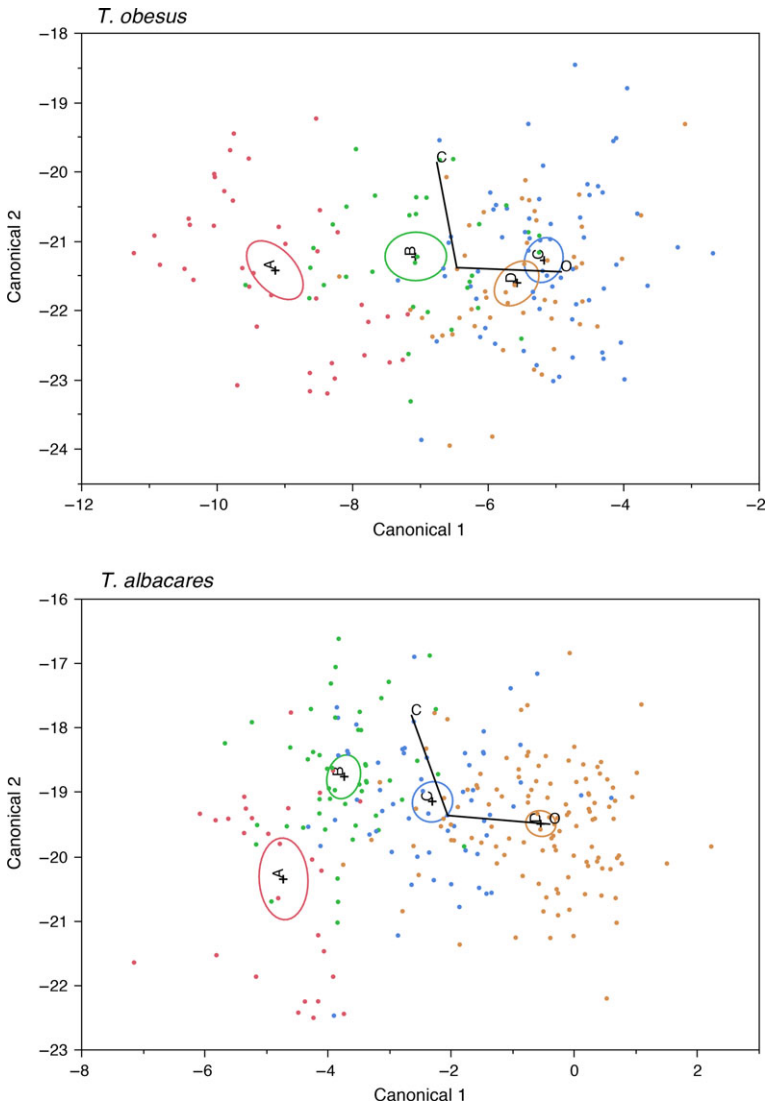

Figure 3. Canonical discriminant analysis (CDA) based on otolith $\delta^{18}O$ and $\delta^{13}C$ for young-of-the-year (YOY) bigeye tuna (*Thunnus obesus)* and yellowfin tuna (*T. albacares*) from the four regions of the western and central Pacific Ocean (WCPO): (A) far west equatorial, (B) west equatorial, (C) central equatorial and (D) Hawaii. Ellipses represent 95% confidence limit around each multivariate mean. Biplot vectors from a grand mean indicate the influence of $\delta^{18}O$ and $\delta^{13}C$ on regional discrimination.

discrimination using this marker alone resulted in a minor reduction to overall classification success to the four regions: *T. obesus* (2%) and *T. albacares* (9%).

Spatial variation in otolith element:Ca ratios of YOY *T. obesus* and *T. albacares* collected in 2008 was also present among the regional nurseries (MANOVA, $P < 0.01$, Table 3 and Fig. 3). The Mg:Ca and Ba:Ca ratios in the otoliths of *T. obesus* from the far west equatorial region were significantly higher than observed for individuals from all other regions sampled (Tukey's HSD, $P < 0.05$), and CDA vectors support the importance of both as being influential in discriminating *T.* obesus from this region (Fig. 4). Mean values of Mg:Ca (639 μmol mol^{-1}) and Ba:Ca (1.0 μmol mol^{-1}) from the far west were at least twofold higher than values observed in the three other regions: Mg:Ca (range: 199–310 μmol mol^{-1}) and Ba:Ca range (range: 0.4–0.5 μmol mol^{-1}). Similarly, otolith Mn:Ca was also highest for *T. obesus* from far west equatorial waters (3.1 μmol mol^{-1}); however, otolith Mn:Ca was statistically similar for individuals from the other equatorial regions but different from individuals from the Hawaii region (1.9 μmol mol^{-1}) (Tukey's HSD, $P < 0.05$). Elemental signatures in the otolith cores of *T. albacares* also varied among the four regions (MANOVA, $P < 0.01$), with multivariate means and 95% CL ellipses from CDA most similar for the far west equatorial and west equatorial regions. Only two of the five element:Ca ratios examined were determined to be influential (Li:Ca and Sr:Ca). Mean otolith Li:Ca for *T. albacares* was significantly lower in

Region	Mg:Ca	Mn:Ca	Sr:Ca	Ba:Ca	N
T. obesus					
A	638 (158)	3.1 (1.5)	1752 (104)	0.96 0(.54)	10
B	310 (250)	2.1 (0.7)	1731 (210)	0.42 (0.21)	25
C	199 (62)	2.7 (1.8)	1698 (200)	0.51 (0.49)	16
D	259 (197)	2.0 (0.6)	1771 (176)	0.41 (0.55)	34

Region	Li:Ca	Mg:Ca	Mn:Ca	Sr:Ca	Ba:Ca	N
T. albacares						
A	5.6 (0.8)	266 (120)	2.3 (0.7)	1750 (80)	0.38 (0.14)	14
B	5.4 (1.0)	208 (153)	2.3 (1.5)	1786 (104)	0.41 (0.10)	24
C	4.5 (1.1)	125 (40)	5.5 (1.9)	1627 (91)	0.51 (0.19)	12
D	5.1 (1.3)	121 (324)	2.3 (1.8)	1620 (282)	0.39 (0.14)	31

A = far west equatorial, B = west equatorial, C = central equatorial, D = Hawaii. All ratios expressed as μmol mol^{-1} and measurements were solution-based (whole otoliths) for *T. obesus* and laser ablation ICP-MS (otolith cores) for *T. albacares*. Li:Ca not determined for YOY *T. obesus*. Sample sizes (N) provided.

Table 3. Mean otolith element:Ca ratios of young-of-the year (YOY) bigeye tuna (*Thunnus obesus*) and yellowfin tuna (*T. albacares*) collected in 2008 from four regions of the West Central Pacific Ocean (WCPO).

the central equatorial (4.5 μmol mol^{-1}) relative to the three other regions investigated (range: 5.1–5.6 μmol.mol^{-1}) (Tukey's HSD, $P < 0.05$). The otolith Sr:Ca also varied regionally with mean values for *T. albacares* from the far west and west equatorial waters (1750 and 1786 μmol mol^{-1}, respectively) being greater than values observed for individuals from the central equatorial (1627 μmol mol^{-1}) or Hawaii (1620 μmol mol^{-1}) regions. For the other three element:Ca ratios examined, mean values were statistically similar among the four regions: Mg:Ca (range: 125–265 μmol mol^{-1}), Mn:Ca (range: 2.3–3.5 μmol mol^{-1}) and Ba:Ca (0.4–0.5 μmol mol^{-1}).

QDFA parameterized with element:Ca ratios in the otoliths of *T. obesus* and *T. albacares* from a single year (2008) indicated that regional discrimination using these markers was lower relative to models based on otolith δ^{18}O and δ^{13}C. Cross-validated classification success for models based on δ^{18}O and δ^{13}C versus element:Ca ratios was higher for both *T. obesus* (60% versus 46%) and *T. albacares* (68% versus 62%). Regional discrimination improved by adding elemental data to models with δ^{18}O and δ^{13}C; nevertheless, overall cross-validated classification success to the four regions only improved slightly with the addition of the elements; *T. obesus* (61%) and *T. albacares* (72%). Given that the addition of elements only improved regional discrimination by 1% to 4% regardless of the ICP-MS approach used [bulk chemistry (whole otolith) versus laser ablation (otolith core)], δ^{18}O appears to represent the most important marker for distinguishing YOY *T. obesus* and *T. albacares* from regional nurseries in the WCPO.

Natal origin

The otolith core δ^{18}O and δ^{13}C values of age-1 and age-2+ *T. obesus* and *T. albacares* collected in 2009 from the west equatorial (Marshall Islands) and Hawaii regions were used to assess the significance of local production and movements for both species. YOY *T. obesus* and *T. albacares* collected in 2008 were used as the baseline sample for mixed-stock predictions, which allowed for age-class matching a fraction of our sample. Age-1 (*c.* 70–100 cm FL) *T. obesus* and *T. albacares* collected in 2009 represented individuals that were 'age-class matched' to the 2008 baseline, and accounted for approximately half (53% and 50%, respectively) of our sample, with the remaining age-2+ tuna probably produced in 2007 or one year earlier than the baseline. Direct MLE estimates for *T. obesus* ($n = 50$) and *T. albacares* ($n = 50$) from the west equatorial waters (Marshall Islands) indicated a limited contribution from other regions (Fig. 5). The predicted contribution (MLE % $\pm$ 1 SD) of *T. obesus* from the three other regions to the west equatorial region was nil (0% $\pm$ 0%) and all recruits originated from nurseries in west equatorial waters, highlighting the importance of local production. Similarly, nearly all of the *T. albacares* in the west equatorial sample were produced in this region (95% $\pm$ 6%), with a minor contribution (5%) derived from the central equatorial region (Line Islands, French Polynesia). MCL estimates were identical for *T. obesus* (100% from a local source) but indicated that the contribution from the central equatorial region may be higher (24% $\pm$ 7%) than predicted with MLE.

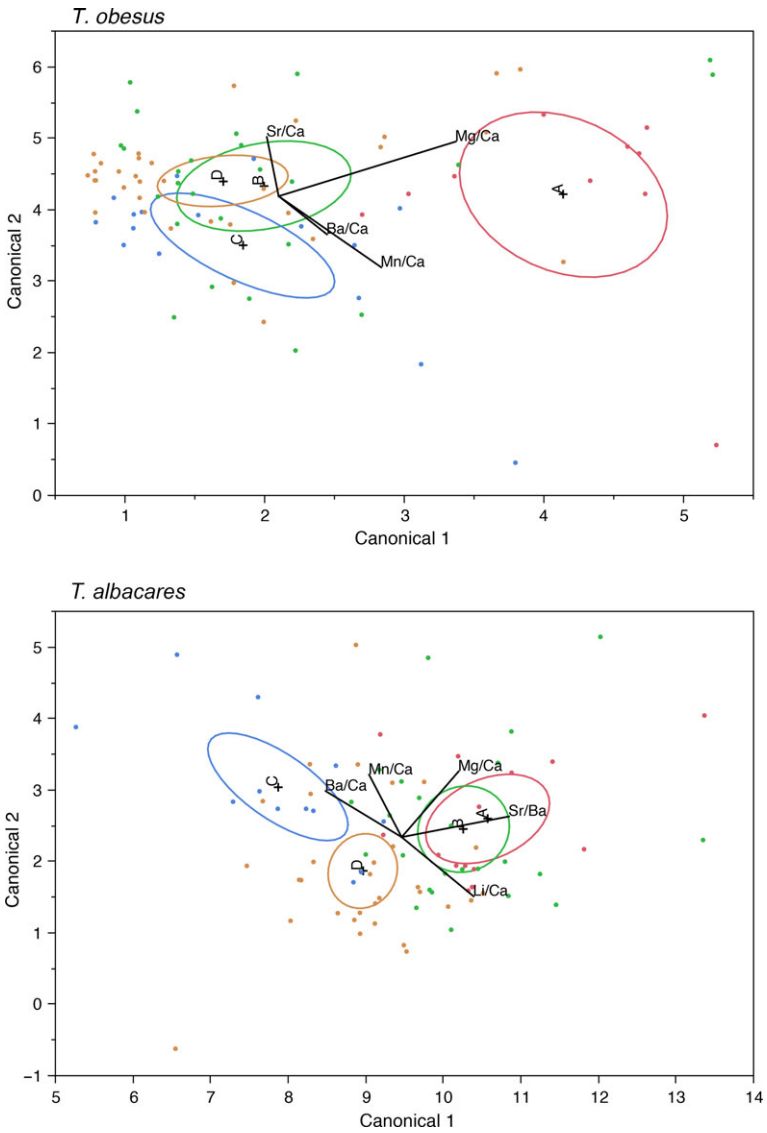

Figure 4. Canonical discriminant analysis (CDA) based on otolith trace elements for young-of-the-year (YOY) bigeye tuna (*Thunnus obesus)* and yellowfin tuna (*T. albacares*) from the four regions of the western and central Pacific Ocean (WCPO): (A) far west equatorial, (B) west equatorial, (C) central equatorial and (D) Hawaii. Ellipses represent 95% confidence limit around each multivariate mean. Biplot vectors from a grand mean indicate the influence of each element:Ca ratio on regional discrimination.

Local production was also important for age-1 to age-2+ *T. albacares* (n = 62) caught in the Hawaii region, and direct MLE estimates indicated that individuals in our Hawaii sample were exclusively produced in the Hawaii region (100% ± 0%), with no contribution from any of the equatorial nurseries (Fig.5). In contrast, the primary source of *T. obesus* (n = 42) in Hawaii was the central equatorial region (65% ± 35%), indicating the potential for significant northward movement of young *T. obesus* from areas south of Hawaii. Only about a third (34% ± 35%) of the *T. obesus* in our Hawaii sample were linked to production from this region. No migrants from the far west or west equatorial regions were detected in the Hawaii sample for either species. It should be noted that error terms from direct MLE estimates of the Hawaii sample were relatively large (*c.* 35%), indicating a high degree of uncertainty associated with our predictions of the natal origin of *T. obesus* in this region. Again, MCL estimates matched MLE for the species showing 100% production from local sources (*T. albacares*); however, MCL indicated that the contribution from local sources in the Hawaii region may be slightly higher (42% ± 36%) than predicted with MLE.

DISCUSSION

Temporal variability in otolith $\delta^{18}O$ and $\delta^{13}C$ was detected for YOY *T. obesus* and *T. albacares* collected in 2008 and 2009, but interannual differences were limited to the far west and west equatorial regions.

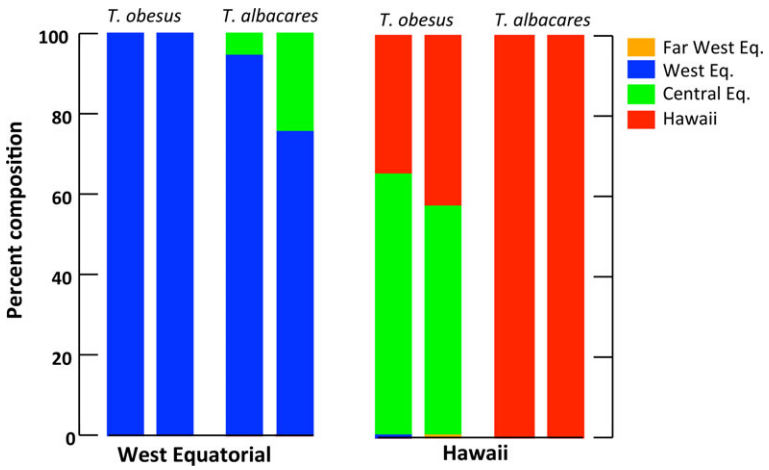

Figure 5. Mixed-stock predictions (percent by region) of natal origin for age-1 to age-2+ bigeye tuna (*Thunnus obesus*) and yellowfin tuna (*T. albacares*) from the two regions of the western and central Pacific Ocean (WCPO): west equatorial and Hawaii. For each species and region, estimates of natal origin are shown in pairs; direct maximum likelihood estimation or MLE (left) and maximum classification likelihood or MCL (right).

Temporal shifts in δ^{18}O for biogenic carbonates are predictably linked to changes in ambient seawater δ^{18}O and temperature (Grossman, 2012). A moderately strong La Niña event was observed in 2007–2008 and this phenomenon resulted in heavy precipitation throughout the far western equatorial region (Lyon and Camargo, 2009; Gordon *et al.*, 2011). In fact, during the winter of 2007–2008, the Philippines experienced the greatest rainfall in nearly four decades, with peak precipitation occurring in early 2008 (Pullen *et al.*, 2015) or after all individuals in our 2008 sample were collected from this region. Increased precipitation in early 2008 from the La Niña event combined with high precipitation again in late 2008 (Pullen *et al.*, 2011) resulted in lower salinities in coastal areas (Gordon *et al.*, 2011). In turn, it appears that both *T. obesus* and *T. albacares* in our 2009 sample were exposed to seawater with depleted δ^{18}O values (rainwater is depleted in ^{18}O relative to seawater), which is in accord with the depleted otolith δ^{18}O values (~0.2‰) observed in 2009. Apart from salinity (δ^{18}O), a sea surface temperature (SST) anomaly was also observed between 2008 and 2009, with mean SSTs during the period approximately 4 months prior to capture (September–December) being about 0.5 °C warmer in 2009 compared to the same period in 2008 (based on cumulative monthly SST data from MODIS/Aqua Global Satellite Level 3, Daytime SST accessed using Marine Geospatial Ecology Tools extension in ArcGIS 10.2; Roberts *et al.*, 2010). Temperature dependence of δ^{18}O is well documented in otoliths and other biogenic carbonates (Grossman and Ku, 1986), and our finding of depleted otolith δ^{18}O with increasing temperature in the Philippines in 2009 is in agreement with the well-documented inverse relationship between otolith δ^{18}O and water temperature (Thorrold *et al.*, 1997; Høie *et al.*, 2003). In response, the combined effects of ocean freshening (lower δ^{18}O) and warmer SST in 2009 for the far west equatorial region appeared responsible for observed temporal shifts in otolith δ^{18}O of both *T. obesus* and *T. albacares*.

Previous studies have reported that the interannual variability in otolith δ^{13}C also occurs for tunas in both the Atlantic Ocean (Rooker *et al.*, 2008b) and Pacific Ocean (Wells *et al.*, 2012), but differences are often variable and add little to the regional discrimination of individuals using these natural tracers (Rooker *et al.*, 2014). For all four regions, otolith δ^{13}C of individuals collected in 2008 and 2009 were statistically similar for YOY *T. albacares*. We did observe a year effect for YOY *T. obesus* from two regions (far west and central equatorial). Nevertheless, as reported previously, linking seawater δ^{13}C directly with otolith δ^{13}C is problematic because dissolved inorganic carbon (DIC) in seawater and a variety of others factors (diet, metabolism and kinetic effects) can ultimately determine the otolith δ^{13}C values (Høie *et al.*, 2003; McMahon *et al.*, 2013).

Regional variation in otolith δ^{18}O was observed for both YOY *T. obesus* and *T. albacares* and maintained even when the 2008 and 2009 cohorts were pooled, signifying that regional differences were sufficiently large enough to overshadow temporal variability within or among the regions examined. Similar to previous research on Atlantic bluefin tuna (*T. thynnus*; Rooker *et al.*, 2014) and Pacific bluefin tuna (*T. orientalis*, Shiao *et al.*, 2010), discrimination of YOY *T. obesus* and *T. albacares* to different geographic regions in the WCPO was due primarily to one marker, otolith δ^{18}O. Otolith δ^{18}O values of both species were the most depleted in the far west equatorial region and increased moving eastward into central equatorial waters. Similar to the aforementioned

explanation of interannual variability, regional differences in seawater $\delta^{18}O$ and temperature appear responsible for observed differences in otolith $\delta^{18}O$ among the four regions. Seawater $\delta^{18}O$ values from the Global Seawater Oxygen-18 Database (v1.21 "http://data.giss.nasa.gov/o18data/) and otolith $\delta^{18}O$ of *T. obesus* and *T. albacares* followed the same pattern in the WCPO. In general, otolith $\delta^{18}O$ values of both species increased moving eastward along the equatorial Pacific (lowest to highest: far west, west and central equatorial). Similarly, both seawater $\delta^{18}O$ (LeGrande and Schmidt, 2006) and sea surface salinity (Delcroix *et al.*, 2011) followed the same west-to-east enrichment pattern continuing northward to the Hawaii region: far west equatorial (lowest), west equatorial, central equatorial and Hawaii (highest). The mean difference in otolith $\delta^{18}O$ between the two geographic end points of our sampling design, the far west equatorial and Hawaii regions, was approximately ~0.8–1.0‰ with otolith $\delta^{18}O$ of YOY tunas being most enriched in the higher salinity waters off the Hawaiian Islands.

Otolith $\delta^{18}O$ is also a known indicator of water temperature experienced by fishes (Kalish, 1991; Thorrold *et al.*, 1997), and its value as a paleothermometer is a result of the strong temperature-dependence of ^{18}O partitioning between the DIC pool and seawater (Grossman, 2012). Therefore, spatial variation in SST among the four regions probably contributed to the observed patterns in otolith $\delta^{18}O$ of YOY *T. obesus* and *T. albacares*. Recently, Kitagawa *et al.* (2013) established a relationship between ambient water temperature and otolith $\delta^{18}O$ for larval Pacific bluefin tuna (*T. orientalis*) and the observed relationship was a 0.27‰ decrease in otolith $\delta^{18}O$ with every 1 °C increase in water temperature over the range investigated. Moreover, comparable temperature-dependent relationships (i.e., slopes) have been reported for several other taxa of marine fishes (e.g., Kalish, 1991; Høie *et al.*, 2004). The estimated cumulative annual mean SST varied markedly among the four regions in 2008 (far west equatorial 29.9°C, west equatorial 29.1°C, central equatorial 26.3°C, and Hawaii 25.3°C), with the two regional end members (far west equatorial and Hawaii) differing by approximately 4.0 °C (based on cumulative monthly SST data at 10 random locations within each sampling region from MODIS/Aqua Global Satellite Level 3). Based on the temperature-otolith $\delta^{18}O$ relationship by Kitagawa *et al.* (2013), this would correspond to an increase of approximately 1.0‰ in the cooler waters of the Hawaii region relative to the far west equatorial region. Observed differences in otolith $\delta^{18}O$ of *T. obesus* and *T. albacares* between the two geographic end points was approximately 0.8‰ and 1.0‰, respectively, with the individuals from Hawaii showing enriched otolith $\delta^{18}O$ as predicted by the otolith $\delta^{18}O$–water temperature relationship. Seawater $\delta^{18}O$ values from each of the regional collection locations are needed from 2008 and 2009 to estimate the relative impact of temperature dependence (Kim *et al.*, 2007). Unfortunately, these data are not available, which limits our ability to assess the relative importance of seawater $\delta^{18}O$ and temperature on observed otolith $\delta^{18}O$ of *T. obesus* and *T. albacares*.

As noted previously, linking seawater $\delta^{13}C$ directly with otolith $\delta^{13}C$ is problematic because other factors can ultimately influence the otolith values (Høie *et al.*, 2003). Similar to other studies examining the otolith $\delta^{18}O$ and $\delta^{13}C$ of tunas at the ocean basin scale (e.g., Wells *et al.*, 2012; Rooker *et al.*, 2014), we observed that spatial variation in otolith $\delta^{13}C$ was minor to inconsequential, even though this marker has shown promise for examining the origin and movement of juvenile fishes from estuarine or coastal nurseries (Thorrold *et al.*, 2001; Mateo *et al.*, 2010). Otolith $\delta^{13}C$ was not influential in discriminating YOY *T. obesus* from the four regions of the WCPO and apart from one region (far west equatorial), otolith $\delta^{13}C$ of YOY *T. albacares* was similar among the other three regions sampled for this species. Discrimination of YOY *T. obesus* and *T. albacares* using this marker alone contributed little to the overall classification success to regional nurseries, suggesting that its value for distinguishing pelagic fishes from different water masses within the WCPO is limited.

Elemental ratios in otoliths have also shown potential for assessing the origin and movement of estuarine, coastal and open ocean fishes (e.g., Gillanders and Kingsford, 1996; Arai *et al.*, 2005; Elsdon and Gillanders, 2006). In the present study, both elements and stable isotopes were quantified for a subset of individuals to evaluate the discriminatory power of each for identifying the origin of YOY tunas inhabiting the WCPO. Spatial variation in certain elements was present for both YOY *T. obesus* and *T. albacares*, with several element:Ca ratios being noticeably higher in certain regions. For *T. obesus*, otolith Mg:Ca, Ba:Ca, Mn:Ca ratios were elevated in the far west equatorial region, and observed differences were not entirely unexpected because hydrography and trace element fluxes vary regionally in the WCPO. Our *T. obesus* sample from the far west equatorial region was based on tuna collected in the southern Philippines (Moro Gulf). This region is heavily influenced by riverine inputs from the Rio Grande de Mindano, which has a

drainage area of over 23 000 km^2 and contains high loads of certain metals (Breward *et al.*, 1996), potentially explaining the observed increase in certain elements (Mg, Mn) in the otolith of *T. obesus* from this region. Concentrations of trace metals in the other, more open ocean regions of the equatorial Pacific (west and central regions) were lower and this is probably because metal concentrations from anthropogenic and lithophilic sources decrease precipitously as the distance from the coastline increases (Bruland and Lohan, 2004). Spatial variation was also detected for YOY *T. albacares* but different element:Ca ratios varied regionally (Li:Ca, Sr:Ca), possibly indicating spatial or temporal partitioning of areas within regional nurseries by the two congeners.

Pronounced regional variation in otolith δ^{18}O resulted in respectable classification success to putative nurseries for both YOY *T. obesus* and *T. albacares* in the WCPO. Models parameterized with otolith δ^{18}O and δ^{13}C indicated that classification to the four regional nurseries was greater for *T. albacares* than *T. obesus*. The cross-validated success of *T. albacares* in 2008 and 2009 (72% and 84%, respectively) was slightly improved over estimates by Wells *et al.* (2012), which did not follow the geographic groupings used in the current study. The classification success of YOY *T. obesus* to the four regions was lower because otolith δ^{18}O values in two of the four regions (central equatorial, Hawaii) overlapped significantly, resulting in a higher number of misclassified individuals and greater uncertainty in mixed-stock predictions of natal origin.

Although otolith chemistry is widely used to assess the origin of tunas and other oceanic fishes, most of the studies to date have focused on δ^{18}O and δ^{13}C signatures (e.g., Wells *et al.*, 2010; Rooker *et al.*, 2014; Fraile *et al.*, 2015) rather than element:Ca ratios, either alone or combined with stable isotopes (e.g. Rooker *et al.*, 2003). We quantified both stable isotopes and element:Ca ratios for a subset of individuals, and this approach shed light on the resolving power of these two classes of natural markers for open ocean species. The cross-validated classification success for models based on stable isotopes only versus element:Ca ratios only were always higher for models parameterized with δ^{18}O and δ^{13}C, and this finding was consistent between the two species. While overall classification success to the different geographic regions improved by adding elemental data to models already parameterized with stable isotopes, the increase in the resolving power was negligible (< 5%). As a result, the effort and cost to incorporate elemental ratios into otolith chemistry baselines for both *T. obesus* and *T. albacares* may not be warranted for future assessments of tuna origin and mixing in the WCPO.

By comparing otolith δ^{18}O and δ^{13}C values of age-1 and age-2+ *T. obesus* and *T. albacares* to our YOY baseline, we determined that both local production and movements influenced the regional composition of fisheries in equatorial waters of the WCPO. For our west equatorial samples of both *T. obesus* and *T. albacares*, all or nearly all individuals (based on MLE: 100% and 95%, respectively) were predicted to be produced from the same region, highlighting the importance of local production and suggesting that longitudinal movements may be limited in this region. Using both conventional and archival tags, Schaefer and Fuller (2009) investigated the movements and dispersion of *T. obesus* in the equatorial eastern Pacific and observed restricted movements and limited dispersion, which is in accord with our finding of retention within the west equatorial waters. More recent studies by Schaefer *et al.* (2015) in the equatorial central Pacific showed regional fidelity but also extensive eastward longitudinal dispersion that was not observed in the present study (i.e., no contribution from far west equatorial waters). Other tagging studies in the Coral Sea (Hampton and Gunn, 1998; Clear *et al.*, 2005) also reported restricted movements and high residency for *T. obesus*. Similar to *T. obesus*, tagging studies on *T. albacares* in equatorial waters also indicated limited longitudinal dispersion (Sibert and Hampton, 2003), supporting our finding that nearly all *T. albacares* in our west equatorial sample were locally produced. A minor contribution of *T. albacares* recruits from central equatorial waters highlights the potential for extended longitudinal movements (> 1000 nmi), which is known to occur for this species (e.g., Davies *et al.*, 2014).

Our estimates of the natal origin for *T. obesus* collected in the Hawaii region indicated the potential for a high degree of south-to-north movement. For *T. obesus* caught in the Hawaii region, otolith chemistry indicated that the primary source of recruits (65%) was not local but rather south of Hawaii, with otolith δ^{18}O and δ^{13}C values matching those of YOY tuna collected in the central equatorial region (Line Islands, French Polynesia). This suggests that large numbers of *T. obesus* migrate northward from southern spawning areas with similar water δ^{18}O values (e.g., north of 10°N); however, it is important to acknowledge that baseline signatures of individuals from Hawaii and the central equatorial regions overlapped, which increased the uncertainty of our predictions (error term 35%). While the majority of age-1 and age-2+ *T. obesus* in our Hawaii sample were

sourced to central equatorial waters, the area between these two regions (10°N to 18°N) may represent a production zone or source of recruits. If individuals from this region possess otolith $\delta^{18}O$ values similar to YOY *T. obesus* from central equatorial waters, predictions of natal origin to this region will be overstated. The potential for an ecologically meaningful contribution of recruits from equatorial nurseries to the Hawaii region has been suggested previously for tropical tunas (Hampton and Fournier, 2001) because production and catch rates in equatorial waters are considerably higher than all other regions in the WCPO (Schaefer *et al.*, 2015). However, a large-scale tagging study by Schaefer *et al.* (2015) in equatorial waters (releases from 5°S to 8°N) showed constrained latitudinal dispersion of *T. obesus* within equatorial waters, with only a few individuals migrating north of 10°N and into the Hawaii region. While the northward movement from the production zone(s) in the south appears to explain our otolith chemistry results, it is difficult to determine the specific latitudinal origin (e.g., south or north of 10°N) of migrants in our Hawaii sample given the spatial structure of our baseline sample. We also observed that approximately one-third of the *T. obesus* in our sample were predicted to originate from the Hawaii region or rather from local production but again our error term is relatively high. Spawning of *T. obesus* occurs over a widespread region of the WCPO, and ichthyoplankton surveys conducted in the Hawaiian Islands have collected *T. obesus* larvae, albeit numbers of larvae are considerably lower than *T. albacares* (Lobel and Robinson, 1988; Nikaido *et al.*, 1991; Paine *et al.*, 2008). The presence of *T. obesus* larvae around the Hawaiian Islands clearly demonstrates that spawning can extend above 15°N and into Hawaiian waters where SST seasonally rise above the spawning threshold (23–24 °C) for this species (Schaefer *et al.*, 2005). However, spawning of *T. obesus* in this region appears to be centered south of the Hawaiian Islands, midway between Hawaii and the Line Islands (Nikaido *et al.*, 1991; Schaefer *et al.*, 2005). While localized spawning or nursery areas in the Hawaiian Islands or possibly from waters immediately to the south the archipelago (south of 19°N) appears to contribute a significant proportion of the *T. obesus* to this region, production farther south appears to be the principal contributor of recruits to the Hawaii region.

In contrast to *T. obesus*, Hawaii was identified as the only source of age-1 to age-2+ *T. albacares* in our sample from this region, suggesting that Hawaiian waters serve as both a production zone and/or nursery area for *T. albacares*. Our results are in accord with tagging studies on *T. albacares* that report restricted movements of this species in the Hawaiian Islands (Dagorn *et al.*, 2007). In fact, Itano and Holland (2000) reported that mean displacement distances of young *T. albacares* in Hawaii were typically less than 50 km from the release location. High fidelity and limited movement of *T. albacares* in Hawaiian waters may be due to the quality/quantity of prey resources and highly suitable habitats (e.g., banks, seamounts) in the region (Wells *et al.*, 2012). Prey availability is often a primary determinant of the movement for pelagic fishes and other marine vertebrates (Forcada *et al.*, 2009; Block *et al.*, 2011; Golet *et al.*, 2013), and the highly suitable habitat experienced by *T. albacares* in Hawaiian waters probably enhances residency and limits their movement. Also, *T. albacares* present in the Hawaiian Islands display a lengthy spawning season from spring to fall when reproductively active adults and larvae have been documented, possibly eliminating the need to migrate elsewhere (Itano, 2000; Paine, *et al.*, 2008). Regardless of the mechanism responsible for retention, our results show that *T. albacares* collected in the Hawaii region were from local sources, indicating that the Hawaii-based fishery for this species is potentially supported by local production with little or no subsidies from equatorial production zones or nurseries.

ACKNOWLEDGEMENTS

Funding for this work was provided by the University of Hawai'i Pelagic Fisheries Research Program (JIMAR project 651106 to JRR). A special thanks to G. Castrence, P. Conley, J. Dettling, D. Dettman, B. Fukuda, D. Fuller, E-J Kim, K. Lind, J. Muir, B. Muller, K. Pollock, K. Schaefer, D. Secor, S. Tobiason, R. Wingate and T. Usu.

REFERENCES

Arai, T., Kotake, A., Kayama, S., Ogura, M. and Watanabe, Y. (2005) Movements and life history patterns of the skipjack tuna *Katsuwonus pelamis* in the western Pacific, as revealed by otolith Sr: Ca ratios. *J. Mar. Biol. Assoc. U.K.* **85:**1211–1216.

Block, B.A., Jonsen, I.D., Jorgensen, S.J. *et al.* (2011) Tracking apex marine predator movements in a dynamic ocean. *Nature* **475:**86–90.

Breward, N., Apostol, A., Appleton, J.D., Gomez, R. and Miguel, J. (1996) Mercury and other heavy-metal contamination associated with gold mining in the Agusan river catchment, Mindanao, the Philippines. BGS Overseas Geology Ser. Tech. Rep. WC/96/61/R: 40.pp.

Bruland, K.W. and Lohan, M.C. (2004) Controls of trace metals in seawater. In: Treatise on Geochemistry — Volume 6: The

Oceans and Marine Geochemistry. H. Elderfield (ed), New York: Elsevier Inc, pp. 23–47.
Chittaro, P.M., Finley, R.J. and Levin, P.S. (2009) Spatial and temporal patterns in the contribution of fish from their nursery habitats. *Oecologia* **160:**49–61.
Clear, N.P., Evans, K., Gunn, J.S., Bestley, S., Hartmann, K. and Patterson, T. (2005) Movement of bigeye tuna (*Thunnus obesus*) determined from archival tag light-levels and sea surface temperatures. In: Migration and Preferences, Habitat of Tuna, Bigeye, Thunnus obesus, on the Coast, East of Australia. Report FRPC, CSIRO 1999/109, pp.19–46.
Dagorn, L., Holland, K.N. and Itano, D.G. (2007) Behavior of yellowfin (*Thunnus albacares*) and bigeye (*T. obesus*) tuna in a network of fish aggregating devices (FADs). *Mar. Biol.* **151:**595–606.
Davies, N., Harley, S., Hampton, J. and McKechnie, S. (2014) Stock assessment of yellowfin tuna in the western and central Pacific Ocean. Western and Central Pacific Fisheries Commission, Document number WCPFC-SC10-2014/SA-WP -04. 112 pp.
Delcroix, T., Alory, G., Cravatte, S., Corrège, T. and McPhaden, M.J. (2011) A gridded sea surface salinity data set for the tropical Pacific with sample applications (1950–2008). *Deep-Sea Res. Pt. I.* **58:**38–48.
Elsdon, T.S. and Gillanders, B.M. (2006) Identifying migratory contingents of fish by combining otolith Sr: Ca with temporal collections of ambient Sr: Ca concentrations. *J. Fish Biol.* **69:**643–657.
Ferriss, B.E. and Essington, T.E. (2011) Regional patterns in mercury and selenium concentrations of yellowfin tuna (*Thunnus albacares*) and bigeye tuna (*Thunnus obesus*) in the Pacific Ocean. *Can. J. Fish Aquat. Sci.* **68:**2046–2056.
Forcada, J., Malone, D., Royle, J.A. and Staniland, I.J. (2009) Modelling predation by transient leopard seals for an ecosystem-based management of Southern Ocean fisheries. *Ecol. Model.* **220:**1513–1521.
Fraile, I., Arrizabalaga, H. and Rooker, J.R. (2015) Origin of Atlantic bluefin tuna (*Thunnus thynnus*) in the Bay of Biscay. *ICES J. Mar. Sci.* **72:**625–634.
Gillanders, B.M. and Kingsford, M.J. (1996) Elements in otoliths may elucidate the contribution of estuarine recruitment to sustaining coastal reef populations of a temperate reef fish. *Mar. Ecol. Prog. Ser.* **141:**13–20.
Golet, W.J., Galuardi, B., Cooper, A.B. and Lutcavage, M.E. (2013) Changes in the distribution of Atlantic Bluefin Tuna (*Thunnus thynnus*) in the Gulf of Maine 1979-2005. *PLoS ONE* **8:**e75480.
Gordon, A.L., Sprintall, J. and Ffield, A. (2011) Regional oceanography of the Philippine archipelago. *Oceanography* **24:**14–27.
Grewe, P.M. and Hampton, J. (1998) An assessment of bigeye (*Thunnus obesus*) population structure in the Pacific Ocean, based on mitochondrial DNA and DNA microsatellite analysis. *CSIRO Mar. Res. No.* **34:**29.
Grewe, P.M., Feutry, P., Hill, P.L. *et al.* (2015) Evidence of discrete yellowfin tuna (*Thunnus albacares*) populations demands rethink of management for this globally important resource. *Sci. Rep.* **5:**16916.
Grossman, E.L. (2012) Oxygen isotope stratigraphy. In: The Geological Time Scale 2012. F. Gradstein, J. Ogg, M. Schmitz & G. Ogg (eds) Oxford, UK: Elsevier, pp. 181–206.
Grossman, E.L. and Ku, T.L. (1986) Oxygen and carbon isotope fractionation in biogenic aragonite: temperature effects. *Chem. Geol.*. Isotope Geoscience Section **59:**59–74.
Hampton, J. and Fournier, D.A. (2001) A spatially disaggregated, length-based, age-structured population model of yellowfin tuna (*Thunnus albacares*) in the western and central Pacific Ocean. *Mar. Freshwater Res.* **52:**937–963.
Hampton, J. and Gunn, J. (1998) Exploitation and movements of yellowfin tuna (*Thunnus albacares*) and bigeye tuna (*T. obesus*) tagged in the north-western Coral Sea. *Mar. Freshwater Res.* **49:**475–489.
Harley, S., Davies, N., Hampton, J. and McKechnie, S. (2014) Stock assessment of bigeye tuna in the western and central Pacific Ocean. In: WCPFC SC10- SA-WP-01, Majuro, Republic of the Marshall Islands, 6–14 August 2014.
Høie, H., Folkvord, A. and Otterlei, E. (2003) Effect of somatic and otolith growth rate on stable isotope composition of early juvenile cod (*Gadus morhua* L.) otoliths. *J. Exp. Mar. Biol. Ecol.* **289:**41–58.
Høie, H., Otterlei, E. and Folkvord, A. (2004) Temperature-dependent fractionation of stable oxygen isotopes in otoliths of juvenile cod (*Gadus morhua L.*). *ICES J. Mar. Sci.* **61:**243–251.
Itano, D.G. (2000) The reproductive biology of yellowfin tuna (*Thunnus albacares*) in Hawaiian waters and the western tropical Pacific Ocean: project summary. In: SOEST. Publ00-01, Joint Institute for Marine and Atmospheric Research (JIMAR) Contribution. Honolulu,HI: JIMAR,pp. 00–328.
Itano, D.G. and Holland, K.N. (2000) Movement and vulnerability of bigeye (*Thunnus obesus*) and yellowfin tuna (*Thunnus albacares*) in relation to FADs and natural aggregation points. *Aquat. Living Resour.* **13:**213–223.
Joseph, J., Squires, D., Bayliff, W. and Groves, T. (2010) Addressing the problem of excess fishing capacity in tuna fisheries. In: Conservation and Management of Transnational Tuna Fisheries.R. Allen, J. Joseph & D. Squires (eds): Blackwell Publishing, pp. 11–38.
Kalish, J.M. (1991) Oxygen and carbon stable isotopes in the otoliths of wild and laboratory-reared Australian salmon (*Arripis trutta*). *Mar. Biol.* **110:**37–47.
Kim, S.T., O'Neil, J.R., Hillaire-Marcel, C. and Mucci, A. (2007) Oxygen isotope fractionation between synthetic aragonite and water: influence of temperature and Mg 2+ concentration. *Geochim. Cosmochim. Ac.* **71:**4704–4715.
Kitagawa, T., Ishimura, T., Uozato, R. *et al.* (2013) Otolith δ18 O of Pacific bluefin tuna *Thunnus orientalis* as an indicator of ambient water temperature. *Mar. Ecol. Prog. Ser.* **481:**199–209.
LeGrande, A.N. and Schmidt, G.A. (2006) Global gridded data set of the oxygen isotopic composition in seawater. *Geophys. Res. Lett.* **33:**L12604.
Lehodey, P. and Leroy, B. (1999) Age and growth of yellowfin tuna (*Thunnus albacares*) from the western and central Pacific Ocean as indicated by daily growth increments and tagging data. WP YFT-2. *SCTB* **12:**16–23.
Lehodey, P., Hampton, J. and Leroy, B. (1999) Preliminary results on age and growth of bigeye tuna (*Thunnus obesus*) from the western and central Pacific Ocean as indicated by daily growth increments and tagging data. Sec. Pac. Com., Oceanic Fish. Prog., 12th meeting, Stand. Com. Tuna Billfish, BET-2: 10 pp.

Lobel, P.S. and Robinson, A.R. (1988) Larval fishes and zooplankton in a cyclonic eddy in Hawaiian waters. *J. Plankton Res.* **10:**1209–1223.

Lyon, B. and Camargo, S.J. (2009) The seasonally-varying influence of ENSO on rainfall and tropical cyclone activity in the Philippines. *Clim. Dynam.* **32:**125–141.

Mateo, I., Durbin, E.G., Appeldoorn, R.S. *et al.* (2010) Role of mangroves as nurseries for French grunt *Haemulon flavolineatum* and schoolmaster *Lutjanus apodus* assessed by otolith elemental fingerprints. *Mar. Ecol. Prog. Ser.* **402:**197–212.

McGarigal, K., Cushman, S. and Stafford, S. (2000) Multivariate Statistics for Wildlife and Ecology Research. New York, NY: Springer-Verlag.

McMahon, K.W., Hamady, L.L. and Thorrold, S.R. (2013) A review of ecogeochemistry approaches to estimating movements of marine animals. *Limnol. Oceanogr.* **58:**697–714.

Millar, R.B. (1987) Maximum likelihood estimation of mixed stock fishery composition. *Can. J. Fish Aquat. Sci.* **44:**583–590.

Millar, R.B. (1990) Comparison of methods for estimating mixed stock fishery composition. *Can. J. Fish Aquat. Sci.* **47:**2235–2241.

Nikaido, H., Miyabe, N. and Ueyanagi, S. (1991) Spawning time and frequency of bigeye tuna, *Thunnus obesus*. *Nat. Res. Inst. Far Seas Fish. Bull.* **28:**47–73.

Paine, M.A., McDowell, J.R. and Graves, J.E. (2008) Specific identification using COI sequence analysis of scombrid larvae collected off the Kona coast of Hawaii Island. *Ichthyo. Res.* **55:**7–16.

Pullen, J.D., Gordon, A.L., Sprintall, J. *et al.* (2011) Atmospheric and oceanic processes in the vicinity of an island strait. *Oceanography* **24:**112–121.

Pullen, J., Gordon, A.L., Flatau, M., Doyle, J.D., Villanoy, C. and Cabrera, O. (2015) Multiscale influences on extreme winter rainfall in the Philippines. *J. Geophys. Res-Atmos.*. doi:10.1002/2014JD022645.

Roberts, J.J., Best, B.D., Dunn, D.C., Treml, E.A. and Halpin, P.N. (2010) Marine Geospatial Ecology Tools: An integrated framework for ecological geoprocessing with ArcGIS, Python, R, MATLAB, and C++. *Environ. Model. Softw.* **25:**1197–1207.

Rooker, J.R., Secor, D.H., Zdanowicz, V.S., De Metrio, G. and Relini, L.O. (2003) Identification of Atlantic bluefin tuna (*Thunnus thynnus*) stocks from putative nurseries using otolith chemistry. *Fish Oceanogr.* **12:**75–84.

Rooker, J.R., Secor, D.H., De Metrio, G., Kaufman, A.J., Rios, A.B. and Ticina, V. (2008a) Evidence of trans-Atlantic movement and natal homing of bluefin tuna from stable isotopes in otoliths. *Mar. Ecol. Prog. Ser.* **368:**231–239.

Rooker, J.R., Secor, D.H., De Metrio, G., Schloesser, R., Block, B.A. and Neilson, J.D. (2008b) Natal homing and connectivity in Atlantic bluefin tuna populations. *Science* **322:**742–744.

Rooker, J.R., Arrizabalaga, H., Fraile, I. *et al.* (2014) Crossing the line: migratory and homing behaviors of Atlantic bluefin tuna. *Mar. Ecol. Prog. Ser.* **504:**265–276.

Schaefer, K.M. (2008) Stock structure of bigeye, yellowfin, and skipjack tunas in the eastern Pacific Ocean. In: Inter-Am. Trop. Tuna Comm. Stock Assess. Rep. 9:203–221.

Schaefer, K.M. and Fuller, D.W. (2009) Horizontal movements of bigeye tuna (*Thunnus obesus*) in the eastern Pacific Ocean, as determined from conventional and archival tagging experiments initiated during 2000-2005. *Inter-Am. Trop. Tuna Comm. Bull.* **24:**191–247.

Schaefer, K.M., Fuller, D.W. and Miyabe, N. (2005) Reproductive biology of bigeye tuna (*Thunnus obesus*) in the eastern and central Pacific Ocean. *Inter-Am. Trop. Tuna Comm. Bull.* **23:**1–31.

Schaefer, K.M., Fuller, D.W. and Block, B.A. (2011) Movements, behaviour, and habitat utilization of yellowfin tuna (*Thunnus albacares*) in the Pacific Ocean off Baja California, Mexico, determined from archival tag data analysis, including unscented Kalman filtering. *Fish. Res.* **112:**22–37.

Schaefer, K.M., Fuller, D.W., Hampton, J., Caillot, S., Leroy, B. and Itano, D. (2015) Movements, dispersion, and mixing of bigeye tuna (*Thunnus obesus*) tagged and released in the equatorial Central Pacific Ocean, with conventional and archival tags. *Fish. Res.* **161:**336–355.

Shiao, J.C., Wang, S.W., Yokawa, K. *et al.* (2010) Natal origin of Pacific bluefin tuna *Thunnus orientalis* inferred from otolith oxygen isotope composition. *Mar. Ecol. Prog. Ser.* **420:**207–219.

Sibert, J. and Hampton, J. (2003) Mobility of tropical tunas and the implications for fisheries management. *Mar. Policy* **27:**87–95.

Sturgeon, R.E., Willie, S.N., Yang, L. *et al.* (2005) Certification of a fish otolith reference material in support of quality assurance for trace element analysis. *J. Anal. Atom. Spectrom.* **20:**1067–1071.

Thorrold, S.R., Campana, S.E., Jones, C.M. and Swart, P.K. (1997) Factors determining δ 13 C and δ 18 O fractionation in aragonitic otoliths of marine fish. *Geochim. Cosmochim. Ac.* **61:**2909–2919.

Thorrold, S.R., Latkoczy, C., Swart, P.K. and Jones, C.M. (2001) Natal homing in a marine fish metapopulation. *Science* **291:**297–299.

Walther, B.D., Thorrold, S.R. and Olney, J.E. (2008) Geochemical signatures in otoliths record natal origins of American shad. *Trans. Am. Fish. Soc.* **137:**57–69.

Ward, R.D., Elliot, N.G., Innes, B.H., Smolenski, A.J. and Grewe, P.M. (1997) Global population structure of yellowfin tuna *Thunnus albacares*, inferred from allozyme and mitochondrial DNA variation. *Fish. Bull.* **95:**566–575.

Wells, R.J.D., Rooker, J.R. and Prince, E.D. (2010) Regional variation in the otolith chemistry of blue marlin (*Makaira nigricans*) and white marlin (*Tetrapturus albidus*) from the western North Atlantic Ocean. *Fish. Res.* **106:**430–435.

Wells, R.J.D., Rooker, J.R. and Itano, D.G. (2012) Nursery origin of yellowfin tuna in the Hawaiian Islands. *Mar. Ecol. Prog. Ser.* **461:**187–196.

Yoshinaga, J., Nakama, A., Morita, M. and Edmonds, J.S. (2000) Fish otolith reference material for quality assurance of chemical analyses. *Mar. Chem.* **69:**91–97.

Young, J.W., Lansdell, M.J., Campbell, R.A., Cooper, S.P., Juanes, F. and Guest, M.A. (2010) Feeding ecology and niche segregation in oceanic top predators off eastern Australia. *Mar. Biol.* **157:**2347–2368.